

Highlights

- A two-stage pyrolysis and thermal or catalytic cracking of MSW was carried out.
- Calcined dolomite was considered as an effective catalyst for syngas production.
- A valuable syngas consisting of more than 80 vol% of CO and H₂ was produced.
- A solid refuse-derived fuel was obtained for further energy requirements.

1
2 **A COMBINED TWO-STAGE PROCESS OF PYROLYSIS AND**
3 **CATALYTIC CRACKING OF MUNICIPAL SOLID WASTE FOR**
4 **THE PRODUCTION OF SYNGAS AND SOLID REFUSE-DERIVED**
5 **FUELS**

6
7 Alberto Veses*, Olga Sanahuja-Parejo, María Soledad Callén, Ramón Murillo, Tomás García
8 Instituto de Carboquímica (ICB-CSIC), C/ Miguel Luesma Castán, 50018 Zaragoza, Spain.

9 **Abstract**

10 Pyrolysis combined to either thermal cracking or catalytic cracking of municipal solid
11 waste was performed in a laboratory-scale facility consisting of a fixed-bed reactor
12 followed by a tubular cracking reactor. The results showed great potential for the
13 production of syngas. The incorporation of inexpensive and widely available dolomite
14 in the cracking reactor (with a constant feedstock to calcined dolomite ratio of 5:1)
15 favoured the catalytic cracking of the primary pyrolysis products towards H₂ and CO in
16 a temperature range of 800–900 °C. More particularly, it was possible at 900 °C to
17 achieve a syngas consisting of more than 80 vol% CO and H₂ with a heating value of 16
18 MJ/Nm³. Additionally, a homogeneous solid fuel was obtained as a solid residue, which
19 can be used to provide additional energy to support the process or as a refuse-derived
20 fuel. Thus, the great potential of this process was demonstrated for turning municipal
21 solid waste into a valuable gas fraction that can be used directly as a fuel or as a source
22 of different value-added products.

23 **Keywords:** Municipal solid waste; pyrolysis; syngas; refuse-derived fuel; calcined
24 dolomite.

25 *Corresponding author: Alberto Veses. Email: a.veses@icb.csic.es. Phone: +34 976
26 733977, Fax: +34 976733318

28 1. Introduction

29 Waste management has emerged as one of the present and future problems of society
30 due to the continuous expansion in volume and complexity of urban and industrial
31 wastes. The eco-friendly processing of municipal solid waste (MSW) will be crucial if
32 we are to overcome the challenge of reducing its social, economic and environmental
33 impact. MSW includes biodegradable waste (food waste, paper, etc.), waste electrical
34 and electronics equipment, recyclable materials (plastics, glass, metals, etc.), hazardous
35 materials (waste tyres, paints, batteries, etc.) and toxic and biomedical waste (Zhou,
36 Long et al. 2015, Sipra, Gao et al. 2018). Currently, about 1.7–1.9 billion tonnes of
37 MSW are generated per year worldwide. This volume is expected to increase to 2.4
38 billion tonnes by 2025.

39 Although a number of countries have significantly increased MSW recycling, reuse and
40 energy recovery, only about a quarter of total MSW is recovered, with the remainder
41 sent to landfills or for incineration (Malinauskaite, Jouhara et al. 2017). These
42 traditional methods of waste disposal are becoming increasingly less viable and, in view
43 of the European Union's Horizon 2020 programme, the amount of waste generated
44 entails not only health hazards and negative environmental impact (greenhouse gases
45 and leaching of waste) but also leaves significant tasks to be dealt with in the future and
46 at great expense. In this regard, new legislation in different countries proposes banning
47 the disposal of MSW in landfills, making the traditional options of landfilling and
48 incineration without energy recovery unviable. Although reduction, reuse and recycling
49 are the main and mandatory steps in the waste management hierarchy, the recovery of
50 value-added products and energy production from thermochemical processes seems to
51 be necessary in order to address the entire waste management process. Thus, the search
52 for new and clean processes that are able to valorise and recover value-added chemicals

53 from waste is seen as a necessity. The latter entails further in-depth investigation into
54 disposal methods and recycling, as well as into new sustainable strategies focused on
55 the valorisation and recovery of waste materials.

56 In this regard, the pyrolysis of MSW is seen as an attractive alternative because it is the
57 only thermochemical process that can produce liquid, solid and gas fractions for direct
58 use either in different power generation facilities or for the production of value-added
59 chemicals (Arena 2012, Chen, Yin et al. 2014). This process results in a more
60 environmentally beneficial process than that of conventional MSW incineration systems
61 since smaller amounts of NO_x and/or SO_x can be released owing to the inert
62 atmosphere used in the process. In addition, the pyrolysis process offers the opportunity
63 to wash the syngas prior to its application (Saffarzadeh, Shimaoka et al. 2006, Wang,
64 Chen et al. 2017), reducing the size and cost of gas cleaning systems, particularly in
65 comparison with state-of-the-art cleaning technology used in incineration facilities. In
66 keeping with this approach, a number of researchers have investigated the process of
67 MSW pyrolysis (Czajczyńska, Anguilano et al. 2017). Most of these works involved
68 studies at laboratory scale, with the feedstock first dried and ground into very small
69 particles and then mixed to obtain a uniform composition. These studies have concluded
70 that temperature and particle size distribution can play a key role in product distribution
71 and selectivity, consistently obtaining a liquid fraction with very poor characteristics.
72 Significantly, high temperature together with small feedstock particle size can
73 significantly enhance gas yields, leading to potential gaseous fuels with a relevant
74 concentration of CO and H₂ and decreasing the yield to the non-valuable liquid fraction
75 (Luo, Xiao et al. 2010, Chen, Yin et al. 2014, Dong, Chi et al. 2016). Therefore,
76 although the pyrolysis process could be an effective waste-to-energy convertor, the low
77 quality of the liquid fraction seems to be a very important issue to be overcome in order

78 to ensure a profitable, clean and comprehensive solution for MSW disposal. The origin
79 of this problem seems to be in the heterogeneous nature of the samples, hampering the
80 production of high quality products, specially a valuable liquid fraction, throughout the
81 optimisation of the process operational conditions.

82 Although a single pyrolysis process would be very attractive from an economical point
83 of view, pyrolysis combined with further gasification technology with air has been
84 proposed as an interesting alternative. Notably, this strategy can be used to increase the
85 yield and characteristics of the gas fraction for its further application as fuel,
86 simultaneously obtaining a homogeneous solid fraction for consideration as a refuse-
87 derived fuel and decreasing the yield of the non-valuable liquid fraction (Chen, Yin et
88 al. 2014, Manyà, García-Ceballos et al. 2015, Aluri, Syed et al. 2018).

89 On the other hand, the addition of catalysts to the process, catalytic pyrolysis, is also
90 proposed to be a very interesting solution for the production of value-added products.
91 For this purpose, several catalysts have been studied in the catalytic pyrolysis of MSW,
92 such as Y-zeolite, β -zeolite, equilibrium FCC, MoO_3 , Ni–Mo catalyst, HZSM-5 and Al
93 $(\text{OH})_3$ in a batch reactor (Ateş, Miskolczi et al. 2013). It has been demonstrated that
94 catalytic pyrolysis does not only increase the yield to the non-condensable gas but it is
95 also enhancing the percentage of valuable products (aromatic and cyclic compounds) in
96 the liquid fraction. More specifically, whilst β -zeolite and HZSM-5 catalysts favours the
97 production of benzene-derived components in the liquid fraction, Ni–Mo-catalysts
98 exhibit the most positive impact to increase H_2 production. Remarkably, although a
99 great part of this H_2 would be produced from fossil fuel derived materials included in
100 MSW, such as plastics, there is an important environmental benefit based on the use of
101 recycled carbon atoms. Though these results looks very promising, the use of low-cost
102 catalysts could be decisive for the economic feasibility of the process, since MSW

103 contains many components, which can deactivate the catalyst during the catalytic
104 pyrolysis process. The excellent performance of calcium-based sorbents for the cracking
105 and reforming of high molecular weight organic components, its widely commercial
106 availability and its relative low price, make these materials very interesting for this aim.
107 Accordingly, other authors (He, Xiao et al. 2010), have studied the catalytic pyrolysis
108 with calcined dolomite. These authors investigated syngas production from this process
109 in a bench-scale fixed-bed reactor over the temperature range of 750–950 °C. The
110 results showed that dolomite had a noteworthy influence on product yields and gas
111 composition, increasing both gas yield and CO / H₂ concentration in the final gas
112 stream. Thus, the obtained gas could be used either as a potential feedstock for Fischer–
113 Tropsch synthesis towards the production of transportation fuels, or as a gas fuel (~ 14
114 MJ/Nm³) in reciprocating engines and gas turbines. On the other hand, O. Tursunov
115 (Tursunov 2014) studied the catalytic pyrolysis of MSW in the temperature range
116 comprised between 200 °C and 750 °C using calcined calcite as calcium-based mineral.
117 This author found that calcined calcite also had a significant positive effect on the yield
118 and composition of the products during the pyrolysis process, particularly by increasing
119 syngas production and decreasing liquid yield. However, it is worth pointing out that
120 there is a very important drawback related to the incorporation of catalysts to the
121 pyrolysis process, since the solid fraction could not be directly commercialized as a
122 refuse-derived fuel and, hence, its use would be limited to provide additional energy to
123 support the process.

124 A very interesting alternative is proposed in this work where the use of cracking
125 catalysts in a second reactor to deal with the vapours generated during the pyrolysis
126 process is investigated. To the best of our knowledge, there is no published data related
127 to syngas production from MSW using this strategy. However, it should be pointed out

128 that notable results have been published by other authors using solely waste plastics
129 (PP, PS or PE) as feedstock (Anuar Sharuddin, Abnisa et al. 2016, Saad and Williams
130 2016, Barbarias, Lopez et al. 2018, Lopez, Artetxe et al. 2018). Significantly, these
131 authors found high conversion efficiencies and H₂ yields using these wastes, that can be
132 found in great quantities in MSW and their production has been increased in late years
133 (López, de Marco et al. 2011, Wu, Chen et al. 2014). We would like to remark that,
134 although the use of a second gasification step of the MSW pyrolysis vapours, using
135 either steam (He, Hu et al. 2009) or air (Chen, Yin et al. 2014), has already
136 demonstrated to be an efficient process configuration to enhance syngas production, the
137 process herein proposed is simpler since the addition of a gasification agent is not
138 needed.. Therefore, this novel configuration could be an alternative thermochemical
139 route for recovering value-added products from MSW especially syngas and refuse-
140 derived fuels, in a simple and low-cost catalytic process using calcium-based materials.
141 In order to accomplish this aim, a study of the influence of the temperature and the
142 incorporation of calcined dolomite and calcined calcite to the process was analysed by a
143 complete characterization of the non-condensable gas production.

144

145 **2. Materials and methods**

146 **2.1 Feedstock**

147 The feedstock used in the current study was obtained from MSW. The sample was
148 provided by the company ECOHISPÁNICA S.A. The industrial pre-processing of the
149 feedstock to make it homogeneous and biologically stable included the following
150 treatments: a) Hydrolysis with saturated steam at 150 °C for 15 min, b) extraction of
151 ferric and non-ferric compounds and other impurities and c) a drying process. Finally,

152 the feedstock was transformed into pellets and used directly. Table 1 summarizes the
153 main properties of the feedstock.

154 Proximate analysis of the received feedstock was determined for moisture content
155 according to the UNE-EN ISO 18134:2016 standard, for ash content according to UNE-
156 EN ISO 18122:2016, and for volatile matter content according to UNE-EN ISO
157 18123:2016. Finally, fixed carbon was determined by balance. Ultimate analysis of the
158 feedstock was determined by Thermo flash 1112, according to the UNE EN 5104
159 standard. The higher heating value (HHV) was measured experimentally with a
160 calorimetric bomb IKA C-2000 using the standard procedure UNE 164001 EX.
161 Calcined dolomite (MgO.CaO) and calcined calcite (CaO) were used as catalysts in this
162 study. MgO.CaO (58% CaO, 36% MgO, Calcinor) and CaO (90% CaO, Calcinor) were
163 commercially available and obtained after the calcination of dolomite and calcite,
164 respectively, at 900 °C. Particle size distribution was in the range of 300–600 µm.

165

166 **2.2. Thermogravimetric analysis**

167 Several thermogravimetric studies were performed in a Netzsch Libra F1
168 thermobalance. First, the thermal behaviour of the initial feedstock under pyrolysis
169 conditions was studied. The thermogravimetric analysis was performed, starting at room
170 temperature, until 700 °C was reached, using heating rate of 30 °C/min.

171 Furthermore, a semi-quantitative thermogravimetric analysis of the calcined dolomite
172 after reaction was conducted. The sample was heated (30 °C/min) in N₂ atmosphere up
173 to 950 °C and kept for 10 min, and the solid weight loss and temperature were recorded.
174 The sample weight used in all experiments was approximately 9 mg and the carrier gas
175 was N₂ (50 mLN/min).

176

177 **2.3 Fixed bed reactor**

178 Pyrolysis + cracking experiments were carried out in a stainless steel fixed-bed reactor
179 (52.5 cm length and 5 cm internal diameter) followed by a tubular reactor (29.5 cm
180 length and 1.5 cm internal diameter), as can be observed in Figure 1. These reactors are
181 heated externally with an electrical resistance heating system. This fixed-bed reactor has
182 the feature of incorporating a vertical mobile liner, where feedstock is deposited. As a
183 result, it is possible to preheat the reactor to the desired temperature while avoiding the
184 contact with the feedstock. Thus, once the required temperature is achieved in the
185 reactor, the liner is introduced into the reaction zone, ensuring the fast heating rates
186 needed for the devolatilisation process. Samples of 25 g were pyrolysed using N₂ as
187 carrier gas (300 ml/min) at 550 °C. The reaction time considered to complete the
188 process was set to 30 min. A tailor-made condenser using a water reflux at 3 °C was
189 used to collect the possible liquid fraction. Liquid fraction was directly recovered by
190 gravity from condenser. Tar fraction was considered the organic fraction deposited
191 along the different parts of the reactor that cannot be collected directly. Thus, the
192 different parts of the installation were weighted and tar was obtained by difference.
193 Finally, the non-condensable gas yield was calculated by the gas composition sampled
194 in a gas bag situated after a filter. Three runs were performed with the setting of 550 °C
195 in the pyrolysis reactor and 700 °C in the cracking reactor, keeping a relative standard
196 deviation (RSD) lower than 5% in product yields. For the remaining experiments, only
197 those with a mass balance of $100 \pm 5\%$ were considered valid. For thermal cracking
198 experiments, different temperatures in the cracking reactor were studied (350 °C, 700 °C
199 and 800 °C) with the setting of 550 °C considered an appropriate pyrolysis temperature.
200 In this case, silica sand was used instead of the catalyst to simulate potential cracking

201 due to the hot particles introduced. The performance of the catalysts was also studied at
202 three different temperatures in the cracking reactor for calcined dolomite (700 °C, 800
203 °C and 900 °C) and at 900 °C for calcined CaO, keeping a constant feedstock/calcined
204 catalyst ratio of 5:1. In addition, several catalytic pyrolysis cycles were performed in
205 order to assess the influence of catalyst regeneration on the yields and quality of the
206 products obtained.

207

208 **2.4 Experimental procedure for cyclic operation**

209 The lifetime activity of the catalyst was also studied. For this purpose, several tests were
210 conducted comprising MSW pyrolysis + catalytic cracking followed by catalyst
211 regeneration in static air (875 °C, 2 h, 30 °C/min). Once accomplished, the catalyst was
212 recovered and reincorporated into the pyrolysis + cracking facility, completing one
213 whole cycle. This process was performed three times, and product characterization was
214 carried out after each experiment, as described in the following section.

215 **2.5 Product characterization**

216 After the pyrolysis + cracking process, tar, solid (char) and non-condensable gas
217 fractions were characterized.

218 The char fraction was analysed by measuring its calorific value (IKA C-2000),
219 elemental composition (Thermo flash 1112) and proximate analysis according to the
220 previously described analytical standards.

221 The chemical composition of the tar fraction was analysed by GC/MS using a Varian
222 CP-3800 gas chromatograph connected to a Saturn 2200 Ion Trap Mass Spectrometer.
223 Firstly, the sample was diluted with 2-propanol and 1µL of sample was injected in split
224 mode with a ratio 20:1. A low bleed capillary column, CP-Sil 8 CB: 5% phenyl, 95%

225 dimethylpolysiloxane (60 m x 0.25 mm i.d. x 0.25 μ m film thickness) was used. An
226 initial oven temperature of 60 °C was maintained for 3 minutes. Then, a ramp rate of 7
227 °C/min was implemented to reach a final column temperature of 300 °C keeping this
228 final temperature for 15.57 minutes. The carrier gas was He (BIP quality) at a constant
229 column flow of 1 mL/min. The injector, detector and transfer line temperatures were
230 300 °C, 220 °C and 300 °C, respectively. The MS was operated in electron ionisation
231 mode within 35-550 m/z range. The interpretation of the mass spectra given by the
232 GC/MS analyses was based on the automatic library search NIST 2011.

233 The non-condensable gases were determined by gas chromatography using a Hewlett
234 Packard series II coupled to a TCD detector. The chromatograph was equipped with a
235 Molsieve 5 Å column to analyse H₂, O₂, N₂ and CO, and with a HayeSep Q column to
236 analyse CO₂ and light hydrocarbons. Both oven programmes used were isothermal at 60
237 °C and 90 °C for the Molsieve and Hayesep Q columns, respectively. Additionally, C1–
238 C4 hydrocarbons were measured through a capillary column in a Varian GC coupled to
239 a FID detector using a temperature programmed method (isothermal at 60 °C for 5
240 minutes, followed by a heating rate of 20 °C/min up to 120 °C, keeping that temperature
241 steady for 5 minutes).

242 **3. Results and discussion**

243 **3.1 MSW fuel properties**

244 As observed in Table 1, the feedstock was characterized by a remarkably high oxygen
245 content (39.9 wt%) and low carbon content (34.7 wt%), implying a low HHV (13.7
246 MJ/kg). It is worth highlighting the relevant amount of volatile matter (53 wt%)
247 observed in the feedstock, making it suitable for devolatilisation processes. This sample
248 is obtained from a mixture of diverse materials such as organic matter, plastics, paper,

249 and metals among others. After steam treatment described in section 2.1 great part of
250 metallic components and plastics are eliminated, whereas organic fraction and
251 hydrolysed paper are remaining as main components. As shown in Table 1, it is worthy
252 of mention the heterogeneous nature in the trace element composition of the stabilized
253 MSW where RSD values ranging from 10 % to 50 % were observed.

254

255 **3.2 Thermogravimetric analyses**

256 Thermogravimetric analysis is a very useful technique to study and understand the
257 pyrolysis behaviour of different feedstocks under well-defined conditions. It is well-
258 known that MSW have an extreme heterogeneity, as they have components similar to
259 organic waste that could be considered as biomass, and other components of a nature
260 similar to what would be plastic waste. The results obtained for weight loss and rate of
261 weight loss for the MSW sample were compiled in Figure 2A. The heterogeneity of the
262 sample could be observed in the existence of several peaks at different temperatures.
263 The first peak at around 100 °C corresponded to the moisture content of the sample. The
264 degradation of the biomass-derived component started at around 200 °C (Navarro,
265 Murillo et al. 2009), followed by the decomposition of plastic-derived materials
266 between 400 °C and 550 °C (Sørum, Grønli et al. 2001, Zhou, Wang et al. 2006, Cabeza,
267 Sobrón et al. 2015). Although after the steam treatment described in previous section, a
268 great part of plastics are eliminated, several plastic-derived components can be clearly
269 appreciated. To confirm this and to offer the reader more information about the nature
270 of this sample several plastics models such as polystyrene or polypropylene and a
271 lignocellulosic biomass model such as pine have been included in Figure 2B. Moreover,
272 550 °C could be a suitable temperature to carry out the complete devolatilisation of this

273 particular MSW since only inert substances and fixed carbon degradation with a very
274 low reaction rate were accounted at temperatures higher than 550 °C.

275 **3.2 Pyrolysis + cracking results**

276 **3.2.1 Product yields**

277 A summary of the product yields of liquid, tar, solid and non-condensable gas fractions
278 after the experiments were reported in Table 2. In all cases, and as expected using the
279 same pyrolysis temperature, char yields remained within the same range (50 wt%
280 approximately) where small differences can be attached to experimental error. With
281 regard to cracking temperature, it should be highlighted that low cracking temperature,
282 350 °C, led to severe operational problems (undesirable heavy waxes formation) and a
283 remarkable proportion of a very low-quality liquid fraction was formed. This liquid
284 fraction presented negligible HHV due to the high oxygen content present (82 wt%) and
285 the low hydrogen and carbon content (6 and 10 wt% respectively). It should be pointed
286 out that, although these results were not included for brevity, experiments carried out
287 fixing up to 550 °C in the cracking reactor produced similar yields. Fortunately, this
288 issue was prevented by using cracking temperatures higher than 750 °C. Thus, as other
289 authors have already stated (Wang, Chen et al. 2017) the increase on the temperature
290 can promote tar cracking by means of several reactions such as decarboxylation,
291 decarbonylation, dehydrogenation, cyclization, aromatization, and polymerization
292 reactions. Under these experimental conditions, gas yield was greatly increased,
293 preventing those negative aspects associated with the production, handling, storage and
294 waste management of the low-quality liquid fraction. Accordingly, gas yield represented
295 up to 25.9 wt% when cracking temperature was set at 700 °C, while it was possible to
296 increase the gas yield up to 35.1 wt% at 800 °C. These results were in line with those

297 obtained by other authors in pyrolysis processes of MSW (Garcia, Font et al. 1995, Luo,
298 Xiao et al. 2010, Dong, Chi et al. 2016) where high process temperatures led to
299 remarkably higher non-condensable gas yields. In comparison with non-catalytic tests, a
300 further increase in non-condensable gases was observed by introducing calcined
301 dolomite into the catalytic cracking reactor, which was nearly 33% and 15% higher
302 when the temperature was set at 700 °C and at 800 °C, respectively. As expected, further
303 increases in the catalytic cracking temperature up to 900 °C led to the highest gas yield
304 (close to 44 wt%), drastically reducing the tar production to 6.8 wt%. These findings
305 followed the general tendency observed in literature (Chen, Yin et al. 2014). After all
306 the experiments, undesirable tar deposition was found in several parts of the reactor.
307 Operational problems related to the formation of this fraction could be considered
308 inherent to reactor configuration and it would be convenient to be reduced, favouring
309 the production of more valuable products. To a better knowledge, this fraction was
310 analysed by GC/MS showing a predominant aromatic nature, where the main
311 components were styrene and benzene-derived compounds such as benzene_1,1'-(2-
312 butene,1,4-diyl)bis- and Benzene_1,1'-(3-methyl-1-propene-1,3-diyl)bis-. These results
313 were in line with TGA analysis where polystyrene could be tentatively identified as one
314 of the main components of the MSW sample. In this line, linear straight-chain alkanes
315 were also identified in tar composition. These compounds could be associated with
316 polypropylene decomposition, which was other main component tentatively identified
317 in the feedstock by TGA. Additional information about the type of compounds can be
318 found in supplementary data.

319 In addition, several pyrolysis-cracking cycles were conducted after regeneration of the
320 catalysts. The pyrolysis and cracking temperatures remained fixed at 550 °C and 900 °C,
321 respectively. It was observed that product yields remained steady at approximately the

322 same values after the cycles, and there was no evidence of catalytic deactivation.
323 Marginal differences in yields could be associated with experimental error.

324 At this point, it should be noted that the cracking activity of CaO was also studied at
325 900 °C (see Table 2). It was observed that the cracking effect was not so evident since
326 there was still a remarkable amount of tar (13.1 wt%). Accordingly, lower gas yield
327 (38.3 wt%) was obtained in comparison with that found using dolomite at the same
328 temperature (43.6 wt%). Although both catalysts could be considered potential
329 candidates to produce a remarkable valuable gas fraction, dolomite shows the greatest
330 potential to enhance gas fraction reducing the operational problems due to tar formation
331 at the same time.

332

333 **3.2.2 Char characterization.**

334 Char properties (proximate and ultimate analysis and heating value) as a mean of all
335 samples analysed were summarised in Table 3. It can be observed that char samples
336 presented low percentages of organic carbon and oxygen, 22.4 wt% and 2.3 wt%,
337 respectively, and a high ash content (73.7 wt%). The low carbon content can be directly
338 linked to the low amount of fixed carbon present in the stabilised MSW. These results
339 entailed a poor heating value, 7.2 MJ/kg. It should be highlighted that significant RSD
340 values were only found in those properties with marginal values. Therefore, it is
341 possible to obtain a relative homogeneous solid fuel, which could be potentially used as
342 an energy source to cover a part of the thermal requirements of the process. Also, given
343 the high ash content of this by-product, its use for other applications such as refuse-
344 derived fuel in cement plants, could be another interesting option. Recently, several
345 researchers (Wang, Chen et al. 2017) have studied the use of the pyrolytic char from
346 MSW as a cracking catalyst. It was demonstrated that the use of this by-product could

347 enhance gas yield and elevate carbon conversion to H₂-rich syngas in catalytic cracking
348 processes, offering another potential alternative for this product and expanding its
349 potential range of application.

350

351 **3.2.3 Non-condensable gas characterization**

352 The non-condensable gas composition was summarised in Figure 3. From that
353 composition, heating value was also calculated and was compiled in Table 4. It must
354 first be pointed out that low cracking temperatures resulted in a CO and CO₂-rich gas
355 where about 65 vol% of the gas consisted of a mixture of both components. CH₄ was
356 the next major component (15 vol%), whereas heavier hydrocarbons (calculated as C₃-
357 C₄) were found in lower proportions (5 vol%). Thus, this composition involved a
358 relatively low LHV of 15.2 MJ/Nm³ (see Table 4). It was observed that increasing the
359 temperature in the cracking reactor up to 700 °C and 800 °C led to a reduction in CO₂,
360 down to 23.2 vol% and 13.9 vol%, respectively. In addition, the CO composition was
361 barely reduced, keeping within the same range of values (approximately 20 vol%). As
362 expected owing to the thermal cracking process, H₂ concentration increased with the
363 temperature, reaching values close to two-fold (33 vol%) in comparison with those
364 found at low temperature. Finally, CH₄ composition could be considered practically
365 constant (from 10.1 vol% up to 13.2 vol%), and heavier hydrocarbons suffered a
366 pronounced increase, approximately three times higher. The final component
367 distribution in non-condensable gas obtained after non-catalytic tests suggests that the
368 main reactions involved are water gas shift reaction (WGS) reaction ($\text{CO}_{(g)} + \text{H}_2\text{O}_{(g)}$
369 $\text{CO}_{2(g)} + \text{H}_{2(g)}$) in combination with hydrogasification ($\text{C} + 2\text{H}_2$ → CH_4) and
370 methanation ($\text{CO} + 3\text{H}_2$ → $\text{CH}_4 + \text{H}_2\text{O}$). These reactions were specially promoted at
371 higher temperatures (800 °C) (Kowalski, Ludwig et al. 2007, Arena 2012, Wang, Chen

372 et al. 2017). These gas composition led to higher heating values, about 28 MJ/Nm³.
373 These values are remarkably higher than those obtained at low temperature, increasing
374 the potential of the fuel gas to be used for power generation. These findings can be
375 considered in line with those obtained from other authors (Chen, Yin et al. 2014). These
376 authors used a complex mixture of feedstock such as wood, paper, polyethylene,
377 municipal plastic waste and crushed MSW in different laboratory-scale pyrolysis plants,
378 showing that both the addition of catalysts and the use of high temperature favoured gas
379 production. Similarly, these authors stated that both syngas production and heating
380 value were maximised at 900 °C.

381 Different tendencies can be highlighted as regards the catalytic cracking experiments.
382 The main tendency that could be observed in Figure 3 was the production of a non-
383 condensable gas with a higher concentration of H₂ and CO as the temperature increased.
384 In this sense, H₂ production increased up to 40.6 vol% and 44.5 vol% at 700 °C and 800
385 °C, respectively. These values implied an increment of more than double in comparison
386 with the non-catalytic test at 700 °C and an increment about 30% at 800 °C. When the
387 cracking temperature was increased to 900 °C, half of the gas stream could be
388 considered H₂ (52.3 vol%). On the other hand, CO also increased, reaching values of up
389 to 33.1 vol% at the highest temperature. Another important parameter that monitored
390 the quality of the product and its potential application was the H₂/CO ratio. Fortunately,
391 H₂/CO ratios between 1.4 and 1.6 were found, which was an optimum range for further
392 applications (Cao, Gao et al. 2008). In addition, it can be highlighted that 82 vol% of
393 the total gas stream consisted of CO and H₂ at 900 °C. With regard to this composition,
394 it could be assumed that WGS reaction in combination with solid-gas reaction between
395 CO₂ and dolomite played an important role, particularly at the highest temperature. In
396 this sense, not only H₂ was maximized, but CO₂ was also minimised and separated from

397 the gas stream in one simple step. Moreover, although several authors have reported that
398 the activity of the Boudouard ($2\text{CO}_{(g)} \rightarrow \text{CO}_{2(g)} + \text{C}_{(s)}$) reaction is lower than that of the
399 WGS reaction (Lim, McGregor et al. 2016), the high temperature involved in the
400 cracking reactor and the presence of CO_2 could enhance CO production through this
401 equilibrium. Indeed, several authors have showed that these two reactions are
402 considered as the main reactions occurring during the devolatilisation of MSW
403 (Kowalski, Ludwig et al. 2007, Arena 2012, Wang, Chen et al. 2017), which are
404 promoted at high temperatures. Particularly, the fact that heavier hydrocarbons are also
405 reduced in the presence of the catalyst, dry reforming ($\text{C}_n\text{H}_m + n\text{CO}_2$
406 H_2) and carbonization ($\text{C}_n\text{H}_{2n+2} \rightarrow n\text{C} + (n+1) \text{H}_2$) reactions seem to be taking place
407 preferentially in presence of the catalyst. These reactions prevail over above mentioned
408 hydrogasification and methanation reactions involved in the no-catalytic process.

409

410

411 A significant environmental issue could be addressed by the reduction of CO_2 and CH_4
412 with the increasing temperature. Thus, CO_2 values of 8.5 vol% and 4.3 vol% and CH_4
413 concentrations of 11.5 vol% and 7.7 vol% were found at 800 °C and 900 °C,
414 respectively. These results suggested that a large proportion of the vapours containing
415 high molecular weight compounds were mainly cracked into light hydrocarbons, CO
416 and H_2 , leading to a significant increase in the gas fraction yield. These results were in
417 line with those obtained by *He et al.* (He, Hu et al. 2009, He, Xiao et al. 2010) where a
418 remarkable increase in H_2 and CO production was also observed as the temperature
419 increased during a catalytic pyrolysis process. Those concentrations were lower than
420 those obtained in the present work and the differences could be attributed to the

421 different nature of the feedstock, reactor design, process configuration and feedstock-to-
422 catalyst ratio.

423 From these results, the significant catalytic effect of the magnesium species in calcined
424 dolomite can be confirmed, improving CO₂ absorption to further increase the
425 concentration of H₂. Although the process is not the same, other authors have observed
426 this effect in biomass gasification (Li, Yang et al. 2017).

427 The composition of the gas fraction was also evaluated after pyrolysis-cracking cycles.
428 It was observed that approximately similar H₂ production was achieved, especially after
429 one cycle conducted, and keeping relevant values after following cycles. CO suffered
430 only a slight reduction, while CO₂ was maintained at low levels, only slightly higher in
431 comparison with the experiment performed with fresh catalyst. Finally, CH₄
432 composition evidenced the opposite trend, increasing its value as cycles were
433 performed. These facts pointed out that a slight catalyst deactivation was taking place
434 after three consecutive cycles but, fortunately, these changes barely affect in a great
435 extent to the gas composition or the heating value. In fact, the H₂/CO ratio was kept at
436 the same value (1.7) after three cycles, preserving its potential for further applications.

437 Another parameter that could be important in order to assess potential gas quality
438 together with the viability of the process is the amount of energy recovery from the
439 initial feedstock. This percentage represents the ratio between the calorific value of the
440 non-condensable gas fraction and the calorific value of the initial feedstock and it is
441 calculated as follows:

442 Although the energy requirements of the thermal processes should be considered, it is
443 worth highlighting that energy recovery values up to 86.5% were obtained when
444 dolomite was used as cracking catalyst at 900 °C, proving that pyrolysis + catalytic
445 cracking could be a clean and simple solution for MSW valorisation.

446

447 **3.3 Thermogravimetric analysis of calcined dolomite**

448 A semi-quantitative thermogravimetric analysis of the spent catalysts were conducted in
449 N₂ atmosphere up to 950 °C, see Figure 4. The thermogram plotted in Figure 4A shows
450 the evolution of different peaks. The first peak at about 400 °C could be related to the
451 dehydration of the calcium hydroxide (Veses, Aznar et al. 2016) inherent to calcium-
452 based materials. The presence of a larger second peak can be also observed with a
453 maximum situated at approximately 750–780 °C. This peak can be associated to the
454 carbonation capacity of the sorbent, which is defining the CO₂ composition of the gas
455 phase. As previously stated, CO₂ concentration seemed to exert a great influence on
456 both WGS and Boudouard equilibriums, which was crucial for both product distribution
457 and composition. Therefore, the evolution of the dolomite carbonation capacity could be
458 the key parameter describing the role of calcined dolomite as cracking catalysts through
459 cycling. Accordingly, several thermogravimetric experiments were conducted on the
460 regenerated catalyst in order to study the CO₂ sorbent capacity of the catalyst. In order
461 to do so, this carbonation stage was performed at 650 °C in a CO₂/N₂ (20/80 vol%)
462 atmosphere. As can be observed in Figure 4B, the CO₂ sorbent capacity of the
463 regenerated catalysts remained approximately within the same range after one cycle.
464 However, it can be observed that the carbonation capacity of the catalysts was reduced
465 as more regeneration cycles were conducted. These features could be related to the

466 sintering phenomena occurring during the regeneration process associated with calcium
467 based catalysts (Martínez, Grasa et al. 2016), decreasing the capacity for CO₂ capture of
468 the sorbent. As expected, this CO₂ sorbent capacity evolution can be considered in line
469 with the results obtained, since gas composition differences were more evident after
470 cycles 2 and 3, as shown in Figure 3. In this regard, CO₂ capture, associated with the
471 CaO contained in dolomite, which simultaneously favours H₂ production via the WGS
472 reaction and the methane reforming reaction, was slightly reduced, and in turn, the role
473 of the catalyst during the upgrading process could be negatively affected, reducing H₂
474 and increasing CO₂ in the gas stream.

475 **3.4 Non-condensable gas applications**

476 By focusing on the results, it is possible to distinguish two main directions. On the one
477 hand, the gas fraction produced at higher temperatures without catalyst is characterised
478 by a relevant heating value, reaching a maximum of 28.1 MJ/Nm³. Thus, this gas could
479 have a huge market, particularly in industrial and domestic boilers where fuel gas is in
480 great demand, or it can be used in gas engines or even gas turbines. On the other hand,
481 the gas obtained after the catalytic process can be considered a derived-syngas for
482 which there is a broad potential market. This gas could be used as syngas for the
483 production of methanol, hydrocarbons, ammonia or transportation liquid fuels through
484 Fischer-Tropsch synthesis (Balat, Balat et al. 2009). Indeed, a stoichiometric H₂/CO
485 ratio ranging from 1 to 2 is commonly utilized in the production of syngas-based
486 chemicals (Cao, Gao et al. 2008). This gas could also be a potential source for the
487 production of H₂, due to its significant content. Although this gas cannot be considered
488 totally renewable, this aspect could have an important environmental impact since
489 approximately about 95% of H₂ comes from fossil fuels, and the share of this product in
490 the energy market is increasing due to the growing demand for zero-emission fuels.

491 Consequently, this H₂ could play a relevant role as a feedstock in the petrochemical,
492 electronics and metallurgical industries (Balat, Balat et al. 2009), as well as a transport
493 fuel. Finally, a special mention should be made of its potential use as a fuel in steam
494 boilers, where its environmental-friendly nature could allow decreasing the cost of gas
495 scrubbing devices.

496

497 **4. Conclusions**

498 A pyrolysis process coupled to either a thermal or a catalytic cracking stage of MSW,
499 was carried out in a laboratory-scale facility consisting of a fixed-bed reactor and a
500 tubular cracking reactor. The results revealed the clear potential of this process for the
501 production of value-added products, particularly that of a valuable gas fraction that can
502 be used directly as a fuel or as a source of different chemicals. The process could be
503 considered cost-effective due to the potential of the obtained char for use as a refuse-
504 derived fuel to contribute to the energy requirements of the process. Moreover, the use
505 of an inexpensive and very widely available catalyst such as calcined dolomite, together
506 with its remarkable catalytic behaviour favouring long-chain hydrocarbon cracking and
507 the formation of H₂ and CO, seems to be a promising alternative. When temperatures of
508 900 °C are reached in the cracking reactor, a syngas is produced with more than 80
509 vol% CO and H₂ and a heating value of 16 MJ/Nm³.

510

511

512 **Acknowledgements**

513 The authors would like to thank MINECO and FEDER for their financial support (Project
514 ENE2015-68320-R). O.S.P acknowledges the FPI fellowship (BES-2016-077750) funded by

515 MINECO. The authors would also like to thank the Regional Government of Aragon (DGA) for
516 the support provided under the research groups support programme.

517

518 **Bibliography**

- 519 Aluri, S., A. Syed, D. W. Flick, J. D. Muzzy, C. Sievers and P. K. Agrawal (2018). "Pyrolysis and
520 gasification studies of model refuse derived fuel (RDF) using thermogravimetric analysis." Fuel
521 Processing Technology **179**: 154-166.
- 522 Anuar Sharuddin, S. D., F. Abnisa, W. M. A. Wan Daud and M. K. Aroua (2016). "A review on
523 pyrolysis of plastic wastes." Energy Conversion and Management **115**: 308-326.
- 524 Arena, U. (2012). "Process and technological aspects of municipal solid waste gasification. A
525 review." Waste Management **32**(4): 625-639.
- 526 Ateş, F., N. Miskolczi and N. Borsodi (2013). "Comparision of real waste (MSW and MPW)
527 pyrolysis in batch reactor over different catalysts. Part I: Product yields, gas and pyrolysis oil
528 properties." Bioresource Technology **133**: 443-454.
- 529 Balat, M., M. Balat, E. Kirtay and H. Balat (2009). "Main routes for the thermo-conversion of
530 biomass into fuels and chemicals. Part 1: Pyrolysis systems." Energy Conversion and
531 Management **50**(12): 3147-3157.
- 532 Barbarias, I., G. Lopez, M. Artetxe, A. Arregi, J. Bilbao and M. Olazar (2018). "Valorisation of
533 different waste plastics by pyrolysis and in-line catalytic steam reforming for hydrogen
534 production." Energy Conversion and Management **156**: 575-584.
- 535 Cabeza, A., F. Sobrón, F. M. Yedro and J. García-Serna (2015). "Autocatalytic kinetic model for
536 thermogravimetric analysis and composition estimation of biomass and polymeric fractions."
537 Fuel **148**: 212-225.
- 538 Cao, Y., Z. Gao, J. Jin, H. Zhou, M. Cohron, H. Zhao, H. Liu and W. Pan (2008). "Synthesis Gas
539 Production with an Adjustable H₂/CO Ratio through the Coal Gasification Process: Effects of
540 Coal Ranks And Methane Addition." Energy & Fuels **22**(3): 1720-1730.
- 541 Chen, D., L. Yin, H. Wang and P. He (2014). "Pyrolysis technologies for municipal solid waste: A
542 review." Waste Management **34**(12): 2466-2486.
- 543 Czajczyńska, D., L. Anguilano, H. Ghazal, R. Krzyżyńska, A. J. Reynolds, N. Spencer and H.
544 Jouhara (2017). "Potential of pyrolysis processes in the waste management sector." Thermal
545 Science and Engineering Progress **3**: 171-197.
- 546 Dong, J., Y. Chi, Y. Tang, M. Ni, A. Nzihou, E. Weiss-Hortala and Q. Huang (2016). "Effect of
547 Operating Parameters and Moisture Content on Municipal Solid Waste Pyrolysis and
548 Gasification." Energy & Fuels **30**(5): 3994-4001.
- 549 Garcia, A. N., R. Font and A. Marcilla (1995). "Gas Production by Pyrolysis of Municipal Solid
550 Waste at High Temperature in a Fluidized Bed Reactor." Energy & Fuels **9**(4): 648-658.
- 551 He, M., Z. Hu, B. Xiao, J. Li, X. Guo, S. Luo, F. Yang, Y. Feng, G. Yang and S. Liu (2009).
552 "Hydrogen-rich gas from catalytic steam gasification of municipal solid waste (MSW): Influence
553 of catalyst and temperature on yield and product composition." International Journal of
554 Hydrogen Energy **34**(1): 195-203.
- 555 He, M., B. Xiao, S. Liu, Z. Hu, X. Guo, S. Luo and F. Yang (2010). "Syngas production from
556 pyrolysis of municipal solid waste (MSW) with dolomite as downstream catalysts." Journal of
557 Analytical and Applied Pyrolysis **87**(2): 181-187.
- 558 Kowalski, T., C. Ludwig and A. Wokaun (2007). "Qualitative Evaluation of Alkali Release during
559 the Pyrolysis of Biomass." Energy & Fuels **21**(5): 3017-3022.
- 560 Li, B., H. Yang, L. Wei, J. Shao, X. Wang and H. Chen (2017). "Absorption-enhanced steam
561 gasification of biomass for hydrogen production: Effects of calcium-based absorbents and NiO-

562 based catalysts on corn stalk pyrolysis-gasification." International Journal of Hydrogen Energy
563 **42**(9): 5840-5848.

564 Lim, J. Y., J. McGregor, A. J. Sederman and J. S. Dennis (2016). "The role of the Boudouard and
565 water–gas shift reactions in the methanation of CO or CO₂ over Ni/γ-Al₂O₃ catalyst." Chemical
566 Engineering Science **152**: 754-766.

567 López, A., I. de Marco, B. M. Caballero, M. F. Laresgoiti, A. Adrados and A. Torres (2011).
568 "Pyrolysis of municipal plastic wastes II: Influence of raw material composition under catalytic
569 conditions." Waste Management **31**(9): 1973-1983.

570 Lopez, G., M. Artetxe, M. Amutio, J. Alvarez, J. Bilbao and M. Olazar (2018). "Recent advances
571 in the gasification of waste plastics. A critical overview." Renewable and Sustainable Energy
572 Reviews **82**: 576-596.

573 Luo, S., B. Xiao, Z. Hu, S. Liu, Y. Guan and L. Cai (2010). "Influence of particle size on pyrolysis
574 and gasification performance of municipal solid waste in a fixed bed reactor." Bioresource
575 Technology **101**(16): 6517-6520.

576 Malinauskaite, J., H. Jouhara, D. Czajczyńska, P. Stanchev, E. Katsou, P. Rostkowski, R. J.
577 Thorne, J. Colón, S. Ponsá, F. Al-Mansour, L. Anguilano, R. Krzyżyńska, I. C. López,
578 A.Vlasopoulos and N. Spencer (2017). "Municipal solid waste management and waste-to-
579 energy in the context of a circular economy and energy recycling in Europe." Energy **141**: 2013-
580 2044.

581 Manyà, J. J., F. García-Ceballos, M. Azuara, N. Latorre and C. Royo (2015). "Pyrolysis and char
582 reactivity of a poor-quality refuse-derived fuel (RDF) from municipal solid waste." Fuel
583 Processing Technology **140**: 276-284.

584 Martínez, I., G. Grasa, J. Parkkinen, T. Tynjälä, T. Hyppänen, R. Murillo and M. C. Romano
585 (2016). "Review and research needs of Ca-Looping systems modelling for post-combustion CO₂
586 capture applications." International Journal of Greenhouse Gas Control **50**: 271-304.

587 Navarro, M. V., R. Murillo, A. M. Mastral, N. Puy and J. Bartroli (2009). "Application of the
588 distributed activation energy model to biomass and biomass constituents devolatilization."
589 AIChE Journal **55**(10): 2700-2715.

590 Saad, J. M. and P. T. Williams (2016). "Catalytic dry reforming of waste plastics from different
591 waste treatment plants for production of synthesis gases." Waste Management **58**: 214-220.

592 Saffarzadeh, A., T. Shimaoka, Y. Motomura and K. Watanabe (2006). "Chemical and
593 mineralogical evaluation of slag products derived from the pyrolysis/melting treatment of
594 MSW." Waste Management **26**(12): 1443-1452.

595 Sipra, A. T., N. Gao and H. Sarwar (2018). "Municipal solid waste (MSW) pyrolysis for bio-fuel
596 production: A review of effects of MSW components and catalysts." Fuel Processing
597 Technology **175**: 131-147.

598 Sørum, L., M. G. Grønli and J. E. Hustad (2001). "Pyrolysis characteristics and kinetics of
599 municipal solid wastes." Fuel **80**(9): 1217-1227.

600 Tursunov, O. (2014). "A comparison of catalysts zeolite and calcined dolomite for gas
601 production from pyrolysis of municipal solid waste (MSW)." Ecological Engineering **69**: 237-
602 243.

603 Veses, A., M. Aznar, M. S. Callén, R. Murillo and T. García (2016). "An integrated process for the
604 production of lignocellulosic biomass pyrolysis oils using calcined limestone as a heat carrier
605 with catalytic properties." Fuel **181**: 430-437.

606 Wang, N., D. Chen, U. Arena and P. He (2017). "Hot char-catalytic reforming of volatiles from
607 MSW pyrolysis." Applied Energy **191**: 111-124.

608 Wu, J., T. Chen, X. Luo, D. Han, Z. Wang and J. Wu (2014). "TG/FTIR analysis on co-pyrolysis
609 behavior of PE, PVC and PS." Waste Management **34**(3): 676-682.

610 Zhou, H., Y. Long, A. Meng, Q. Li and Y. Zhang (2015). "Classification of municipal solid waste
611 components for thermal conversion in waste-to-energy research." Fuel **145**: 151-157.

612 Zhou, L., Y. Wang, Q. Huang and J. Cai (2006). "Thermogravimetric characteristics and kinetic of
613 plastic and biomass blends co-pyrolysis." Fuel Processing Technology **87**(11): 963-969.

614 **TABLES**

615 **Table 1.** Main properties of stabilized MSW as received. Left: proximate analysis,
 616 ultimate analysis and heating value. Right : trace elements.

| Property | Values | RSD (%) | Trace elements (wt. %) | Values | RSD (%) |
|---------------------------------|--------|---------|------------------------|--------|---------|
| Proximate analysis (wt%) | | | Al | 2.61 | 13.4 |
| Moisture | 3.7 | 5.9 | Ca | 17.9 | 15.8 |
| Ash | 37.1 | 2.6 | Fe | 1.46 | 37.5 |
| Volatile matter | 52.5 | 2.3 | K | 3.09 | 41.0 |
| Fixed Carbon | 6.6 | 6.3 | Mg | 1.70 | 28.8 |
| | | | Mn | 0.06 | 35.8 |
| Ultimate analysis (wt%) | | | Na | 3.88 | 25.8 |
| C | 34.7 | 5.8 | P | 1.01 | 18.4 |
| H | 4.6 | 5.1 | Si | 18.8 | 15.8 |
| N | 1.5 | 6.5 | Ti | 0.29 | 17.5 |
| S | 0.4 | 5.4 | | | |
| O* | 39.9 | 10.6 | | | |
| LHV (MJ/kg) | 12.7 | 3.4 | | | |

617 *Calculated by difference

618

619 **Table 2.** Product yields (liquid, tar, solid and non-condensable gas) after the pyrolysis +
 620 cracking of MSW.

| Experimental conditions (T _{Pyrolysis} - T _{cracking} - Catalyst) | Yields (wt%) | | | | |
|--|--------------|------------|------------|---------------------|-------|
| | Liquid | Tar | Char | Non-condensable gas | Total |
| 550 °C-350 °C | 6.1 ± 0.1 | 25.3 ± 1.2 | 50.1 ± 0.8 | 14.3 ± 0.6 | 95.8 |
| 550 °C-700 °C | 0.0 ± 0.0 | 22.1 ± 0.9 | 49.3 ± 1.0 | 25.6 ± 1.0 | 97.0 |
| 550 °C-800 °C | 0.0 ± 0.0 | 14.5 ± 0.6 | 49.3 ± 1.0 | 35.6 ± 1.2 | 99.4 |
| 550 °C-700 °C-Dolomite | 0.0 ± 0.0 | 8.7 ± 0.3 | 49.8 ± 0.9 | 39.1 ± 1.2 | 97.5 |
| 550 °C-800 °C-Dolomite | 0.0 ± 0.0 | 8.5 ± 0.4 | 49.7 ± 1.0 | 41.0 ± 1.2 | 99.3 |
| 550 °C-900 °C-Dolomite | 0.0 ± 0.0 | 6.8 ± 0.7 | 49.0 ± 1.1 | 43.6 ± 1.4 | 99.4 |
| 550 °C-900 °C-Dolomite - Cycle 1 | 0.0 ± 0.0 | 7.7 ± 0.3 | 49.5 ± 0.9 | 42.5 ± 1.3 | 99.7 |
| 550 °C-900 °C-Dolomite - Cycle 2 | 0.0 ± 0.0 | 8.7 ± 0.4 | 48.1 ± 1.1 | 41.1 ± 1.2 | 98.0 |
| 550 °C-900 °C-Dolomite - Cycle 3 | 0.0 ± 0.0 | 7.8 ± 0.3 | 48.1 ± 1.1 | 41.8 ± 1.3 | 97.7 |
| 550 °C-900 °C-Calcined calcite | 0.0 ± 0.0 | 13.1 ± 0.8 | 48.7 ± 1.0 | 38.3 ± 1.0 | 96.3 |

621

622

623 **Table 3.** Proximate analyses, ultimate analyses and heating value of char after pyrolysis
 624 + cracking process of MSW.

| Property | Char (at 550°C) | RSD (%) |
|---------------------------------|-----------------|---------|
| Proximate analysis (wt%) | | |
| Ash | 73.7 | 0.8 |
| Volatile matter | 13.2 | 3.6 |
| Fixed Carbon | 10.8 | 4.6 |
| Ultimate analysis (wt%) | | |
| C | 22.4 | 1.6 |
| H | 0.4 | 25.4 |
| N | 0.6 | 9.1 |
| S | 0.7 | 13.1 |
| O | 2.3 | 31.5 |
| LHV (MJ/kg) | 7.1 | 2.0 |

625

626

627

628

629 **Table 4.** Heating value (MJ/Nm³) of gas stream calculated from gas composition

| Experimental conditions (T _{Pyrolysis} - T _{cracking} - Catalyst) | Non-condensable gas | | Energy recovery from initial feedstock (%) |
|--|---------------------------|-------------|--|
| | LHV (MJ/Nm ³) | LHV (MJ/kg) | |
| 550 °C-350 °C | 15.2 | 11.9 | 12.8 |
| 550 °C-700 °C | 26.5 | 23.6 | 45.3 |
| 550 °C-800 °C | 28.1 | 31.0 | 80.7 |
| 550 °C-700 °C-Dolomite | 22.5 | 28.4 | 82.3 |
| 550 °C-800 °C-Dolomite | 17.0 | 24.4 | 74.0 |
| 550 °C-900 °C-Dolomite | 16.1 | 26.8 | 86.4 |
| 550 °C-900 °C-Dolomite - Cycle 1 | 18.1 | 26.7 | 84.2 |
| 550 °C-900 °C-Dolomite - Cycle 2 | 16.0 | 25.5 | 77.5 |
| 550 °C-900 °C-Dolomite - Cycle 3 | 15.9 | 24.9 | 77.3 |

630

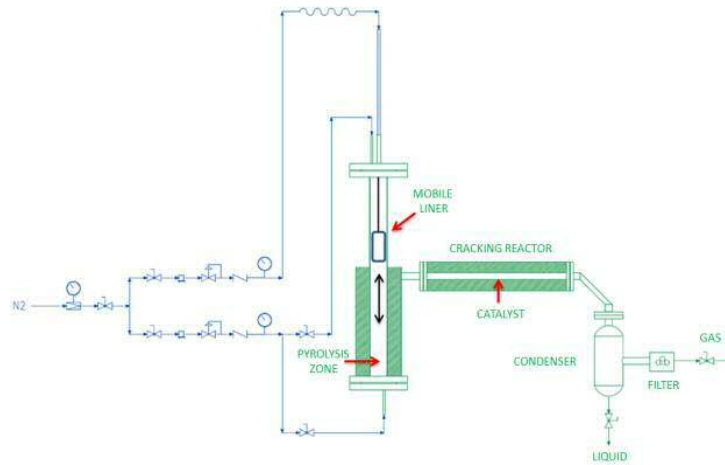
631

632

633

634 **FIGURES**

635



636

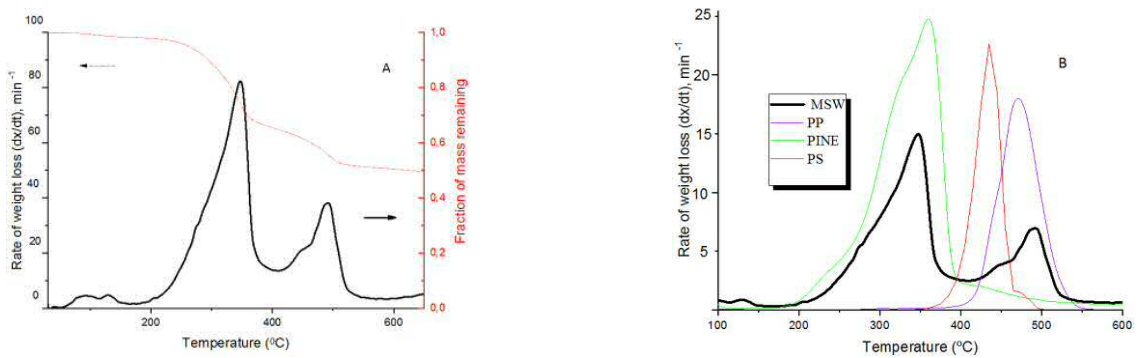
637 **Figure 1.** Schematic diagram of the fixed-bed reactor used for determining co-pyrolysis performance.

638

639

640

641



642

643 **Figure 2.** Thermogravimetric results of A: MSW (weight loss and rate of mass loss), and B: MSW (black), pine
644 (green), polystyrene (red) and polypropylene (blue) at 30 °C/min.

645

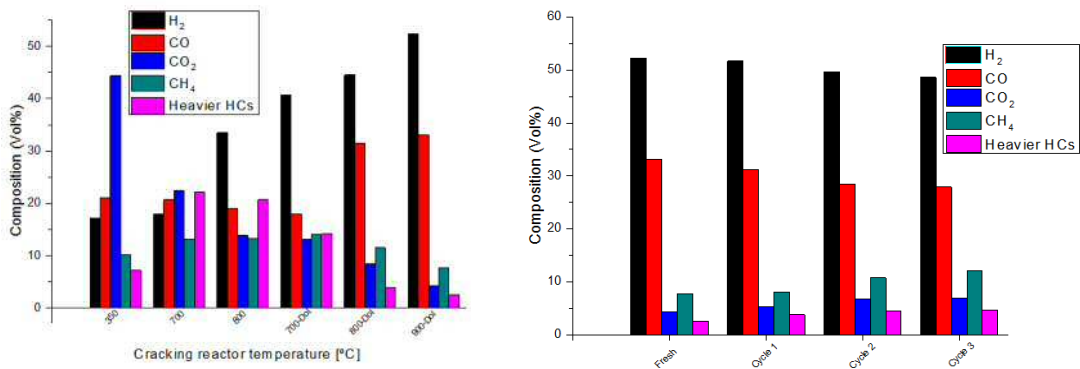
646

647

648

649

650



651

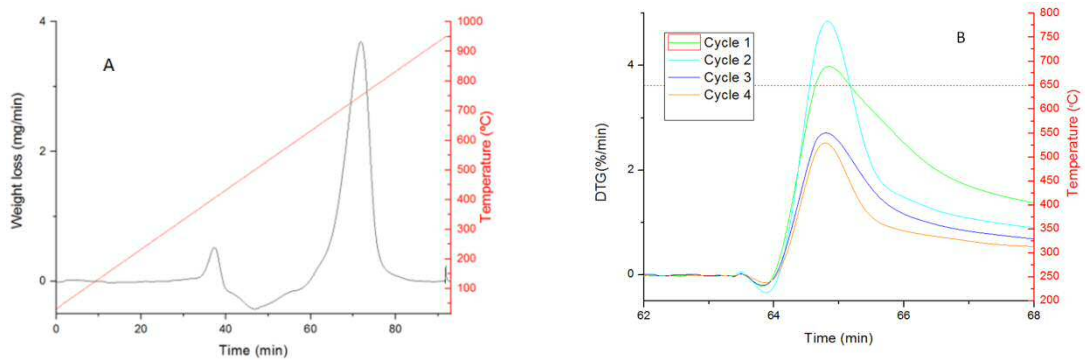
652 **Figure 3.** Left: Gas composition (vol %) after pyrolysis + cracking and catalytic cracking of
653 MSW at different temperatures. Right: Gas composition (vol %) after several catalytic pyrolysis
654 + cracking cycles at 900 °C.

655

656

657

658



659

660 **Figure 4.** Thermogravimetric analysis of calcined dolomite after pyrolysis + catalytic cracking
661 of MSW. Figure A shows the weight loss and temperature represented over time. Figure B
662 shows the carbonation capacity of the catalysts after regeneration cycles.

663